

Jerzy KOTKOWSKI, Edward ROKICKI, Paweł LINDSTEDT,
 Jarosław SPYCHAŁA, Jerzy PERCZYŃSKI, Hieronim KARBOWIAK
Air Force Institute of Technology (Instytut Techniczny Wojsk Lotniczych)

DIAGNOSTICS OF TURBINE BLADES, BASED ON ESTIMATION OF FREQUENCY RESPONSE FUNCTION

Diagnostyka łopatek turbinowych w oparciu o oszacowanie funkcji odpowiedzi częstotliwościowej

Abstract: *The aim of the study is to propose a diagnostics method based on blade's vibration model in frequency domain. Amplitude spectrum $A(\omega)$ and phase spectrum $\varphi(\omega)$ have been experimentally identified which define transfer function $G(j\omega) = P(\omega) + jQ(\omega)$ and their real $P(\omega)$ and imaginary $Q(\omega)$ parts. Transfer function $G(j\omega)$ and resulting frequency, amplitude, phase characteristics and real $P(\omega)$ and imaginary $Q(\omega)$ parts are parts of blade's diagnostics model. Changes in those characteristics are directly related to changes in the technical condition of the blades. It has been noticed that small changes in the technical condition cause large changes in frequency characteristics, which proves their usefulness in the diagnosis process.*

Keywords: modal analysis, blade vibration, frequency response, resonance, Bode plot, vibration mode, operating deflection shape, Q factor, vibration spectrum, transfer function, frequency response function

Streszczenie: *Celem badania jest zaproponowanie metody diagnostycznej opartej na modelu drgań łopatek w dziedzinie częstotliwości. Zidentyfikowano eksperymentalnie widma amplitudowe $A(\omega)$ i fazowe $\varphi(\omega)$, które definiują transmitancję operatorową $G(j\omega) = P(\omega) + jQ(\omega)$ oraz jej rzeczywiste $P(\omega)$ oraz urojone $Q(\omega)$ części. Transmitancja operatorowa $G(j\omega)$ i wynikająca z niej częstotliwość, amplituda, charakterystyka fazowa oraz rzeczywiste $P(\omega)$ i urojone $Q(\omega)$ części są częściami modelu diagnostycznego łopatki. Zmiany w tych charakterystykach są bezpośrednio związane ze zmianami w stanie technicznym łopatek. Zauważono, że małe zmiany w stanie technicznym powodują duże zmiany w charakterystykach częstotliwościowych, co świadczy o ich przydatności w procesie diagnostycznym.*

Słowa kluczowe: analiza modalna, drgania łopatek, reakcja na częstotliwość, charakterystyka Bodego, tryb drgań, kształt odchylenia roboczego, współczynnik Q , spektrum drgań, transformacja operatorowa, funkcja odpowiedzi częstotliwościowej

1. Introduction

Rotating blades are critical components of an aircraft turbine engine, power turbines and wind turbines. They work in extremely difficult and varying load conditions. These difficult working conditions result in that the blades are subject to premature fatigue, resulting in the appearance of micro-crack and then tear off of the portion of the blade leaf. Minimizing the threat to the safety of engine operation requires periodic inspection of the technical condition of the blades. Experience in the testing and inspection of blades implies that it is difficult to identify higher forms of vibrations in damaged blades. In the standard repairs it assumed that the control of the blades is carried out by conventional NDT methods (flaw detection, fluorescent, magnetic, eddy current). They allow the identification of late stage blades damage. Monitoring of blade vibration using the existing "tip timing" algorithms also gives very ambiguous results.

The control carried out on a mechanical inductor with laser measurement does not ensure the excitation of real operating higher forms of vibration of the blade, hence only in the case of finding a deviation in the frequency of the first mode from the technical conditions, the blade airfoil is subjected to tune. Practice shows that the controlled natural vibration frequency of the first mode and its Q factor certainly do not determine the blade technical condition accurately enough and can only be treated as important parameters and auxiliary information.

Frequency identification methods of the object are used in diagnosis of the blade in a relatively small range. The frequency characteristics of the blade, in each case, are sensitive to changes in object parameters, and what is most important, can be experimentally determined with incomplete information about the input and output of the blade.

Only full control of the oscillation frequency and Q factor in a wide spectrum of vibration can give a more detailed view of the technical condition of the blades. The course of phase amplitude characteristics and response times are a good indicators of changes in blade technical condition.

2. Theoretical basis of the description of the blade

The blade is a technical object with a very complex operation. It is described by a linear mathematical model in the form of differential equations determined its response to extortion.

The following assumption has been made:

1. input signals are a combination of periodic, harmonic and polyharmonic functions
2. output signals are also a combination of periodic, harmonic and polyharmonic functions but amplified and shifted by the offset phase φ in relation to the input signals

3. the relation between the input and output signals is described by spectral transmittance

where: $G(j\omega) = A(\omega)e^{j(\varphi_\omega)}$

$A(\omega)$ – amplification of spectral transmittance

$\varphi(\omega)$ – phase offset of spectral transmittance

Models described by systems of differential equations can be converted to algebraic operator models. The most popular of them are transformations based on Laplace (L) and Fourier (F) integral transforms.

Thus, the differential equation is as follows:

$$b_m y^{(m)}(t) + \dots b_n y(t) + b_0 y(t) = a_n x^{(n)}(t) + \dots a_n x(t) + a_0 x(t) \quad (1)$$

It can be reduced by the Laplace transformation to an algebraic operator equation:

$$b_m s^{(m)} y(s) + \dots b_n s y(s) + b_0 y(s) = a_n s^{(n)} x(s) + \dots a_n s x(s) + a_0 x(s) \quad (2)$$

Based on (2), function $H(s)$ is transmittance and is defined as the ratio of the transform of the output function $Y(s)$ to the transform of the input function $X(s)$:

$$G(s) = \frac{Y(s)}{X(s)} = \frac{b_m s^{(m)} y(s) + \dots b_n s y(s) + b_0 y(s)}{a_n s^{(n)} x(s) + \dots a_n s x(s) + a_0 x(s)} \quad (3)$$

Transmittances arising on the basis of differential equations have the form of rational functions, while in most real objects the numerator degree is smaller than the denominator degree of the transmittance function. Based on the transmittance $G(s)$ and the transform of the input function $X(s)$, the transform of the output function can be determined as follows:

$$Y(s) = G(s)X(s) \quad (4)$$

hence the original of the output function can be reproduced $y(t)$.

Usually, this is not necessary, because basic tests of object properties (stability, equilibrium point) can be performed based on transmittance. The stability of the system is determined by the transmittance poles, i.e. the roots of the characteristic equation of the system determined by matching the transmittance denominator to zero (denominator roots):

$$a_n s^{(n)} + \dots a_n s + a_0 = 0 \quad (5)$$

This object is stable if all the poles have a negative real part. Zero transmittance does not affect system stability. It is assumed that the model of the blade describing its dynamics will be its transmittance. It involves transform input signals, which are all operating extortion, transform output signals, which signals are her answers. Input (x) and output (y) signals are tested, measured in time domain (t). It can be analyzed equivalently in the time domain (t) or in the frequency domain (f).

According to the control theory, it can be assumed that the blade is an object of the automation system (fig. 1), on which the input signal $x(t)$ acts as an element of the set, it converts it into the output signal $y(t)$ as an element of the other set.

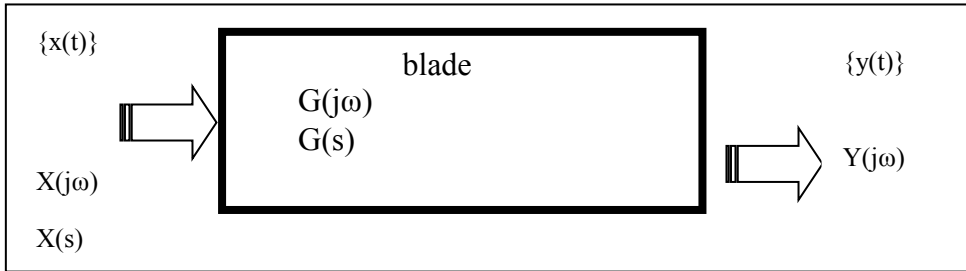


Fig. 1. The blade as the automation object, $H(s)$ – operator transmittance, $H(j\omega)$ – spectral transmittance $s=j\omega$, t – time, s – complex variable, $j\omega$ – imaginary variable

In addition, we assume that the input signal is described in the field of complex numbers and has the following form:

$$x(t) = A_x(\cos(\omega t) + j \sin(\omega t)) = A_x(\omega)e^{j\omega t} \quad (6)$$

where: $A_x(\omega)$ – amplitude,
 ω – frequency.

It is also assumed that the output signal $y(t)$ is described in the domain of complex numbers and has the following form:

$$y(t) = A_y(\cos(\omega t + \varphi) + j \sin(\omega t + \varphi)) = A_y(\omega)e^{j(\omega t + \varphi)} \quad (7)$$

where: $A_y(\omega)$ – amplitude,
 ω – frequency,
 φ – phase relative to the input signal.

The signal $x(t)$ and $y(t)$ describe physical quantities and thus satisfy the sufficient condition for the existence of equivalent Fourier transforms $X(j\omega)$ and $Y(j\omega)$ [2].

Thus, the blade as an automation object can be described by spectral transformation [1, 5, 14, 15]:

$$G(j\omega) = \frac{b_m(j\omega)^m + \dots b_0}{a_n(j\omega)^n + \dots a_0} = A(\omega)e^{j(\varphi(\omega))} = \frac{Y(j\omega)}{X(j\omega)} \quad (8)$$

where:

b_0, b_1, \dots, b_m – transformation parameters related to its ‘zeros’,

a_0, a_1, \dots, a_n – transformation parameters associated with its ‘poles’,

$A(\omega)$ – amplitude gain,

$\varphi(\omega)$ – phase shift.

In spectral transmittance we can distinguish the real part of the transmittance $P(\omega)$ and the imaginary part $jQ(\omega)$. We can write:

$$G(j\omega) = P(\omega) + jQ(\omega) \quad (9)$$

Since

$$G(j\omega) = A(\omega)e^{j(\varphi(\omega))} \quad (10)$$

That

$$|G(j\omega)| = A(\omega) = \sqrt{P^2(\omega) + Q^2(\omega)} \quad (11)$$

$$\varphi = \text{arctg} \frac{Q(\omega)}{P(\omega)} \quad (12)$$

The $x(t)$ signal is any superposition of harmonic and polyharmonic signals and its result can be not only periodic signals but also signals, that are not periodic, but having the characteristics of periodic signals.

$$x(t) = \sum_{n=1}^{\infty} a_k (\cos(k\omega_1 t + \varphi_k) + j \sin(k\omega_1 t + \varphi_k)) \quad (13)$$

$$x(t) = \sum_{k=1}^n a_k (\cos(k\omega_1 t + \varphi_k) + j \sin(k\omega_1 t + \varphi_k)) \quad (14)$$

$$x(t) = A_1 \sin(\omega_1 t) + A_2 \sin(\omega_2 t) + A_3 \sin(\omega_1 t) \cos(\omega_3 t) \quad (15)$$

Equations (11 and 12) are the basis for determination of the fundamental frequency characteristics: amplitude – fig. 2a, phase – fig. 2b and amplitude-phase – fig. 3 [12].

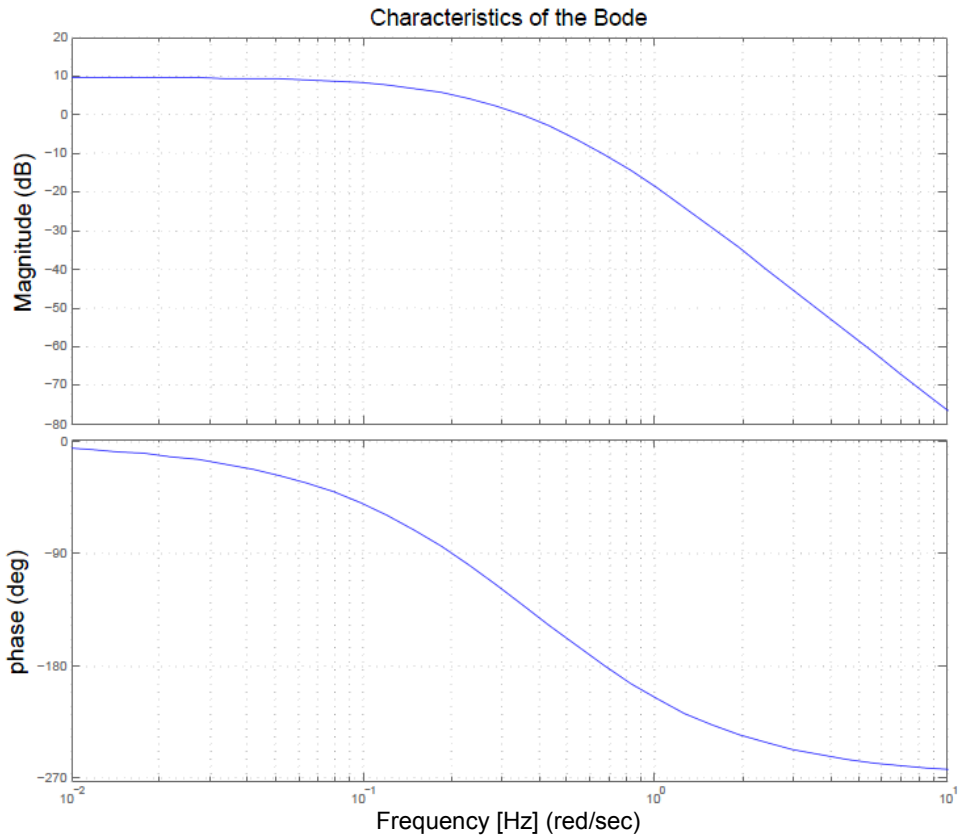


Fig. 2. Bode plots

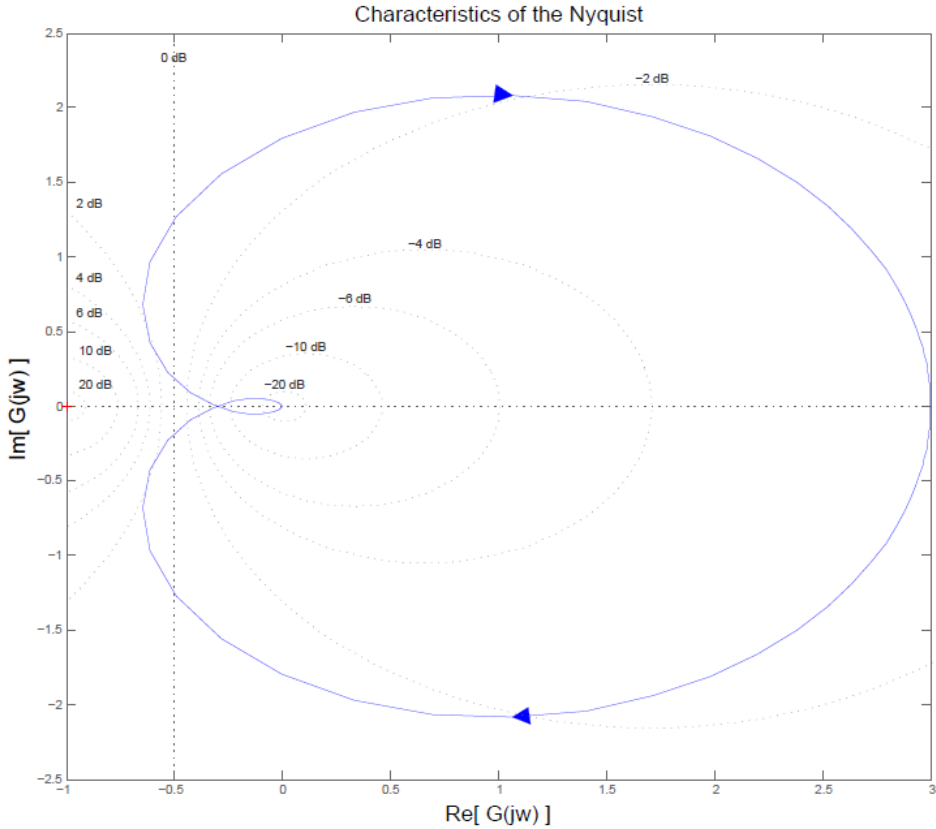


Fig. 3. The characteristics of the Nyquist in Matlab

The fact that the phase-amplitude characteristic only describes the relationship between the $\{x(t)\}$ and $\{y(t)\}$ signals means that it can also be determined in case of incomplete information about the $\{x(t)\}$ and $\{y(t)\}$ signals [11].

We assume in the model that multi-resonance vibrations correspond to the parallel RLC resonance circuit, vibrations related to the flow of the working medium are described by the transmittance of the minimum phase object, taking into account its interaction with the other blades in the blade rim. Each blade's degree of freedom has a different natural frequency and is defined as the resonance frequency of the degree of freedom.

Amplitude amplifications of subsequent modes of the second degree of freedom are in the form of and are further components of the blade's transmittance:

$$A_{\omega} = \sum_{k=1}^m A_k e^{-j\beta_k(\omega-\omega_k)} \quad (17)$$

ω_k – the resonant frequency of the second states of their own degree of freedom,
 β_k – the blade transmittance parameter associated with the blade material properties.
 The general form of transmittance after all own states of all degrees of freedom:

$$A_\omega = \sum_{k=1}^{\infty} A_k e^{-j\beta_k(\omega-\omega_k)} + \sum_{i=1}^{\infty} A_i e^{-j\beta_i(\omega-\omega_i)} + \dots \sum_{w=1}^{\infty} A_w e^{-j\beta_{wh}(\omega-\omega_{wh})} \quad (18)$$

Where h is another degree of freedom

$$\beta_w(\omega - \omega_w) > 6$$

Accepted condition

$$\text{For each } \left| \frac{\omega - \omega_w}{\beta_w} \right| > \frac{6}{\beta_w} \quad A_w \Rightarrow 0$$

From the equation, we conclude the general form of the phase characteristics of the blade:

$$[A_\omega, \varphi_\omega] = f\left(\sum_{k=1}^{\infty} A_k e^{-j\beta_k(\omega-\omega_k)} + \sum_{i=1}^{\infty} A_i e^{-j\beta_i(\omega-\omega_i)} + \dots\right) \quad (19)$$

Accepted next condition

$$\text{For each } \left| \frac{\omega - \omega_w}{\beta_w} \right| > \frac{6}{\beta_w} \quad \varphi_w \Rightarrow 0$$

In the diagnosis process, the characteristics $P(\omega)$, $Q(\omega)$ and amplitude - phase characteristics $G(j\omega) = A(\omega)e^{j(\varphi_\omega)}$ are of particular importance. The experimentally determined amplitude phase characteristics help to study the forms of blade vibration. The real part $P(\omega)$ of the phase-amplitude characteristic $H(j\omega)$ can also be determined. $P(\omega)$ will be used to obtain time characteristics such as e.g. step response:

$$h(t) = \frac{2}{\pi} \int_0^{\infty} \frac{P(\omega) \sin(\omega t)}{\omega} d\omega \quad (20)$$

The transmittance component $P(\omega)$ is directly related to the step response $h(t)$ formula (16) and impulse response $g(t) = \frac{dh(t)}{dt}$. Thus, a direct relationship of the signals $A(\omega)$ and $\varphi(\omega)$ measured during the movement of the blades with the signals $h(t)$ and $g(t)$ characterizing the blade during rest is obtained. $P(\omega)$ allows to determine the natural frequency range determining the frequency response [1, 6].

$$\frac{P(\omega)}{P(0)} \leq 0.1 \div 0.2$$

And also that $P(\omega)$ the large ω determines the nature of the $h(t)$ waveform for small t times. Full information about the dynamics of the automation object is included in the amplitude - phase characteristics (fig. 3), which is determined on the test rig.

Finally, it can be stated that the amplitude-phase characteristic allows you to effectively identify performance indicators, the course of the amplitude, phase characteristics, response time technical condition by testing changes in the parameters of the quality indicators of the transmittance of the object, which in our case is the blade.

The analysis of blade signals from the shaker allowed to determine the model in which the blade is an element of automation with many degrees of freedom. Its degrees are associated with multi-resonant bending, torsional vibrations and vibrations related to the flow of the working center.

The object identification based on the phase-amplitude characteristic obtained experimentally consists in comparing it with the reference graph. From here one can determine the order of the differential equation, resonance frequencies, zeroes and poles and its parameters, as well as the delay, relations between poles and zeroes of transmittance [1, 10, 11].

3. The description of test bench of the ND37 blade

In ITWL, an inductor has been built forcing the vibration of the blade, which is the input signal $x(t)$ – fig. 4. It possible to study the blade behavior by examining the output signal $y(t)$ generated by the blade as part of the blade response set in the range from 0 Hz to 20 kHz. We have a record of $\{x(t)\}$ and $\{y(t)\}$ signals. We also determine the phase shift between these signals.

The basic components of the position (fig. 4) are as follows:

- generator Zopan PO-28 nr NC/2008/0175
- Virtual Bench VI-8012
- measuring amplifier WQ-4
- battery with 2 gel accumulators 12V / 12Ah
- electromagnetic inductor
- exciter mounting stand
- vice for fixing the blade
- Asus G73J
- NI 9239 measuring module
- NI USB-9162 module
- BNC coaxial cables - 9 pcs
- set of 4 piezoelectric sensors
- SVAN 948 vibration meter



Fig. 4. The view of the ND37 blade measuring stand

The view of the ND37 blade on the measuring stand is presented in fig. 5.



Fig. 5. The view of the ND37 blade on measuring stand

Signal measurements were based on authoring software. Figure 6 shows a view of the front panel VI F Fast Sw4Ch FFT with the FFT window. It measures amplitude of vibration and the Q factor of the blade for all resonances obtained. Figure 7 shows a view of the front panel of the VI F Slow Sweep 4Ch.

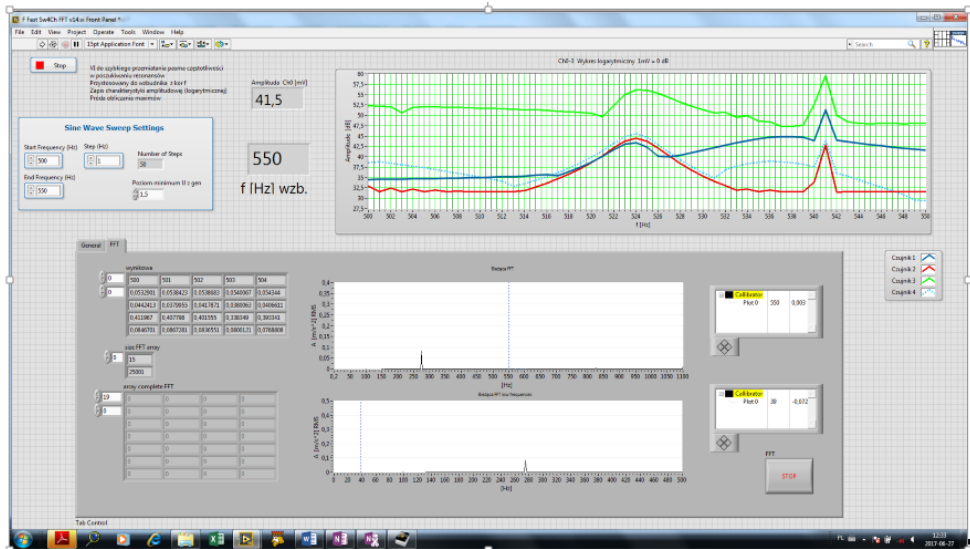


Fig. 6. The view of the front panel VI F Fast Sw4Ch FFT with the FFT window

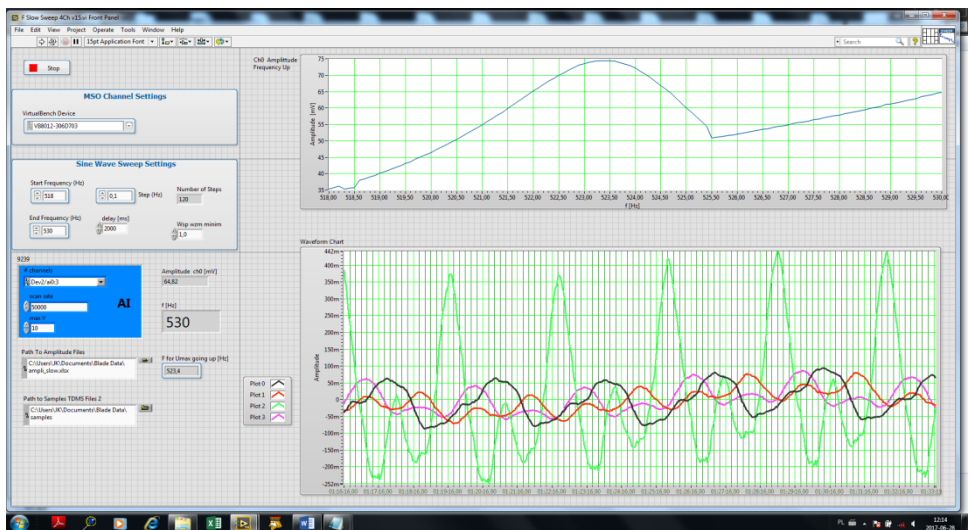


Fig. 7. The view of the front panel of the VI F Slow Sweep 4Ch

It accurately measures the amplitude of the maximum vibration amplitude and blade Q factor in the selected frequency range.

The measuring stand also allows determining the excited vibration form of the blade in the vibration phase analyzer option illustrated in fig. 6.

4. Examples of test bench results

Test results are presented in the form of frequency characteristics. These are the amplitude $A(\omega)$, phase $\varphi(\omega)$ characteristics, the real part of the spectral transmittance $P(\omega)$, the imaginary part of the spectral transmittance $Q(\omega)$ and the synthesis amplitude - phase characteristics $G(j\omega)$. Figure 8 shows the amplitude characteristics of the ND37 blade in the band up to 6kHz.

The time series of the $x(t)$ and $y(t)$ signals allowed for the determination of the blade phase characteristics. Examples of signals are shown in figs. 9, 10 and 11. The inductor tests show that the blade has multi-resonant phase-amplitude characteristics. The characteristic test is incomplete because the influence of the working medium flow on the phase amplitude characteristic is omitted. No flow does not allow testing the full working characteristics of the blade at our stand. The final characteristic will also have the distribution of the wave function in the spin region. This will be the next stage of our research. In the working conditions of the inductor we obtained coarse amplitude characteristics of fig. 8 and accurate in narrow ranges for the example of figs. 12 and 13.

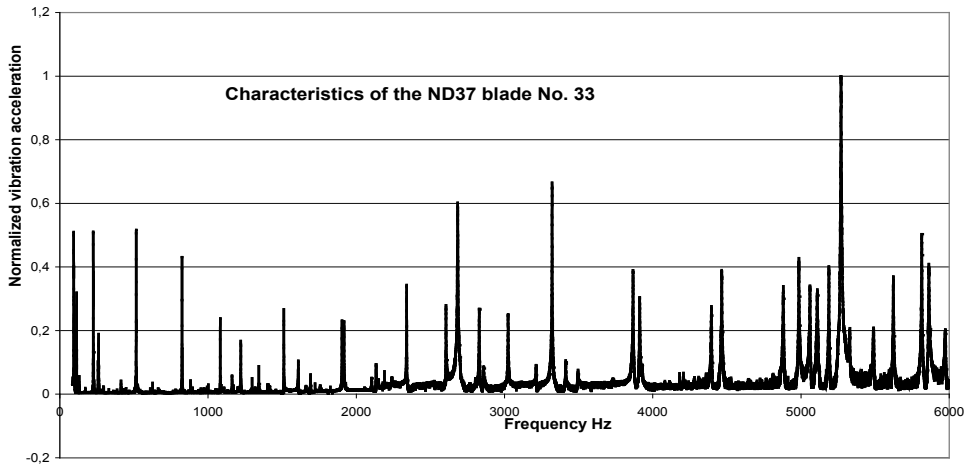


Fig. 8. The amplitude characteristics $|Y(\omega)|$ on ND37 blade obtained on an ITWL inductor in the band up to 6 kHz

Figures 11, 12 and 13 show 3 graphs from a set of hundreds of graphs to determine the phase shift between the $x(t)$ and $y(t)$ signals. The charts for 1079 Hz, 1081.4 Hz and 1084 Hz were selected.

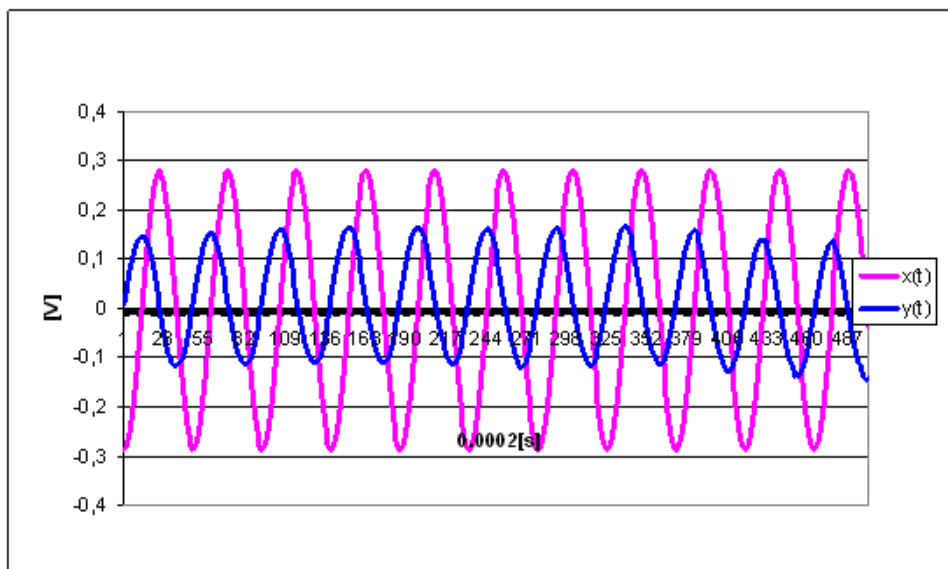


Fig. 9. The time course of force $x(t)$, the output signals $y(t)$ with frequencies 1079 Hz

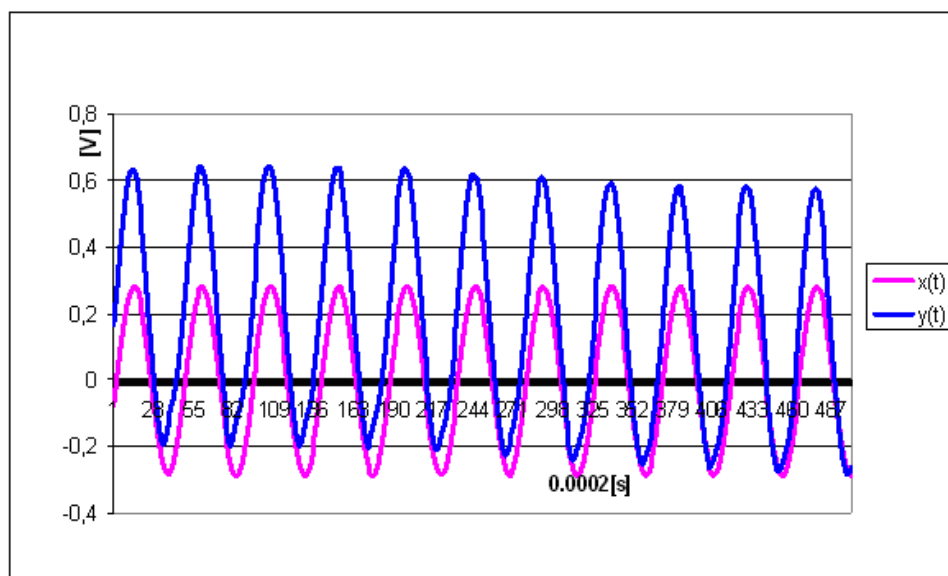


Fig. 10. The time course of force $x(t)$, the output signals $y(t)$ with frequencies 1081,4 Hz

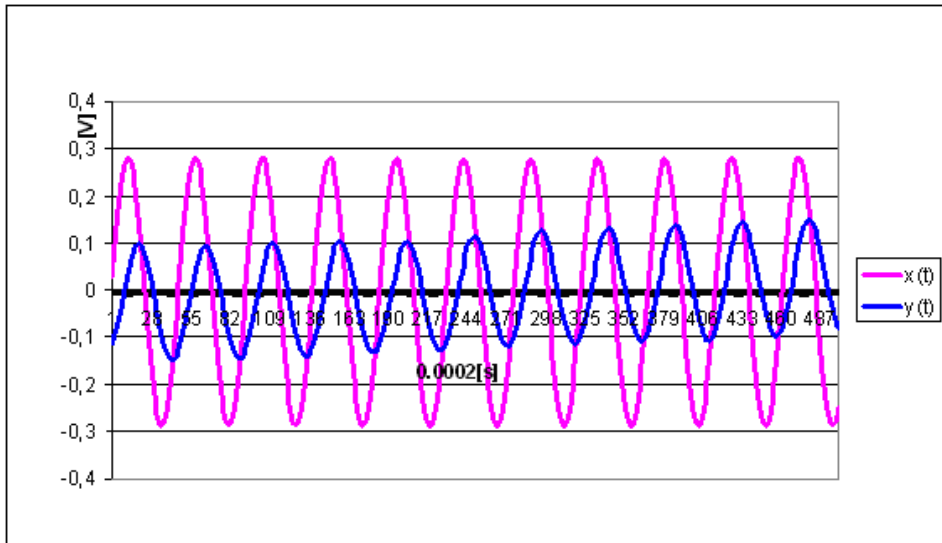


Fig. 11. The time course of force $x(t)$, the output signals $y(t)$ with frequencies 1083,7 Hz

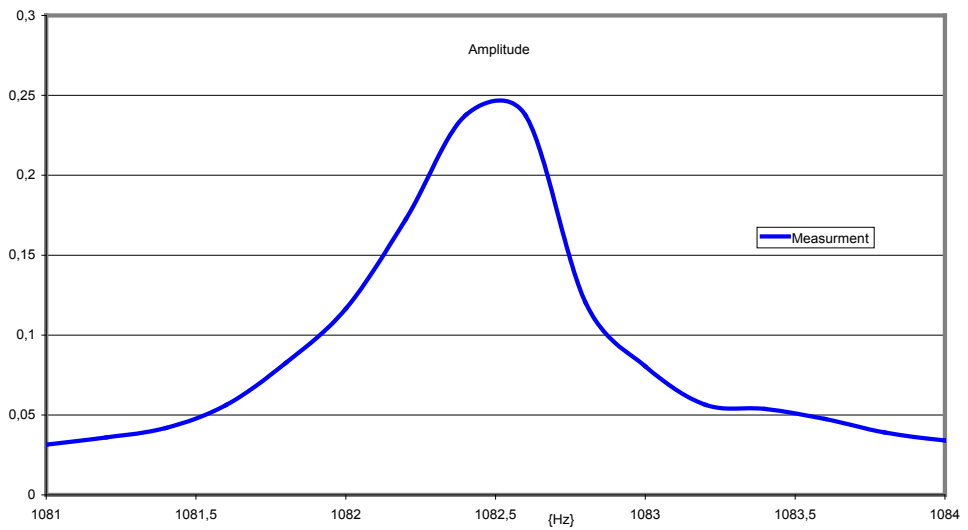


Fig. 12. The frequency characteristics of spectral transmittance $|Y(\omega)|$ of the ND37 blade near 1082 Hz

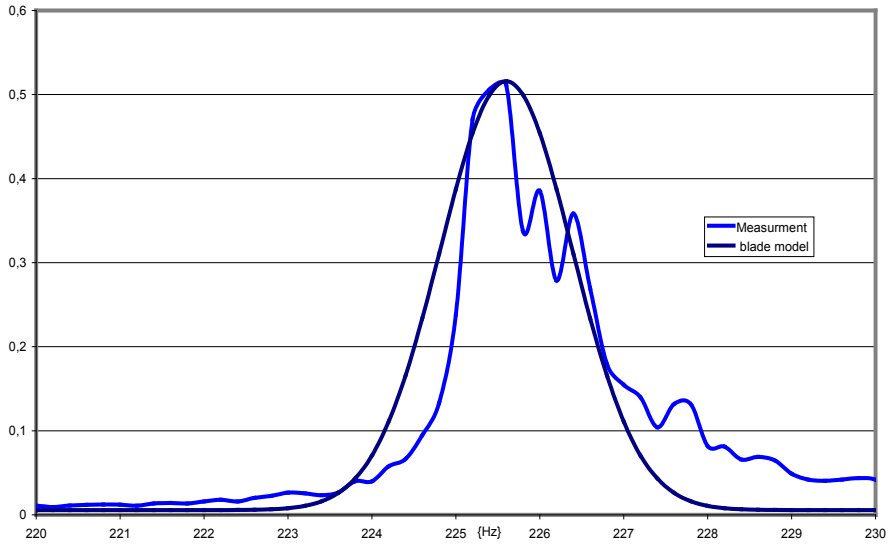


Fig. 13. The frequency characteristics of spectral transmittance $|Y(\omega)|$ of the ND37 blade near 225 Hz

Compared to the model and the actual measurement, fig. 13 shows the effect of phase and Q factor transmittance blades for a response to a stimulus. Due to the fact that the inductor changes the frequency of excitation, there is a delay in blade response. In turn, when leaving the resonance, oscillations appeared typical for the study of high-quality resonance transmittance. For the measuring range from fig. 13, the phase characteristics were measured and it is shown in fig. 14.

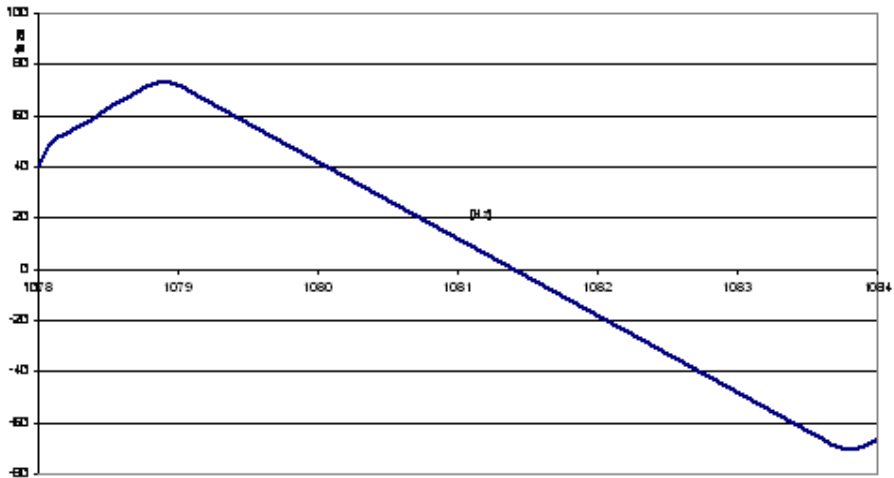


Fig. 14. The phase characteristics between $x(t)$ and $y(t)$ signals for the ND37 blade measured a test bench near the frequency of 1082 Hz

5. Conclusion

Based on the results of experimental research, the object (element - blade) is identified as a multi-resonant broadband automation system. The initial identification of the system was carried out on the measuring stand. It has been confirmed that for full identification, the excitation signal should be modified to improve its correlation with the actual excitation signal. A mathematical model is created, followed by a diagnostic model. It has been shown and noticed that the most faithful model of a blade operating in a very complex environment described by the signal $\{x(t)\}$ [4, 7, 9, 12] is the spectral transmittance $G(j\omega)$, the resulting frequency characteristics and the real $P(j\omega)$ and imaginary part $Q(j\omega)$ of the spectral transmittance $G(j\omega)$.

6. References

1. Antoniewicz J.: Automatyka. WNT. (in Polish) Warszawa 1973.
2. Beauchamp K.G.: Przetwarzanie sygnałów metodami analogowymi i cyfrowymi. WNT. (in Polish) Warszawa 1978.
3. Bodner W.A.: Automatyka silników lotniczych. WMON. (in Polish) Warszawa 1958.
4. Bracewell R.: Przekształcenie Fouriera i jego zastosowania. WNT. (in Polish) Warszawa 1968.
5. Findeisen W.: Automatyka. Poradnik Inżyniera. WNT. (in Polish) Warszawa 1973.
6. Franks L.E.: Teoria sygnałów. PWN. (in Polish) Warszawa 1975.
7. Grądzki R., Borowczyk H., Lindstedt P.: Parametryczna metoda diagnozowania łopatk z eliminacją niemierzalnych czynników otoczenia. Problemy Badań Eksploatacji Techniki Lotniczej. Tom 8. Wyd. ITWL. (in Polish) Warszawa 2012.
8. Kotowski A., Lindstedt P.: The using of signals of impulse acoustic response in tests of rotor blades in stationary conditions. ISCORMA 4 Calgary Alberta Canada 2007.
9. Krasowski A.A., Pospiełowski G.S.: Podstawy automatyki i cybernetyki technicznej. WNT. (in Polish) Warszawa 1965.
10. Kurowski W.: Podstawy teoretyczne komputerowego miernictwa systemów mechanicznych. Wydawnictwa Politechniki Białostockiej. (in Polish) Białystok 1994.
11. Maksimov W., Jegorov N., Karasev W.: Izmerenije, obrabotka i analiz bystroprimiennych processow w maszynach. (in Russian: Measurement, treatment and analysis quick changing processes in machines) Maszynostrojenije, 1987.
12. Osowski J.: Zarys rachunku operatorowego. WNT. (in Polish) Warszawa 1982.
13. Pelczewski W.: Teoria sterowania. WNT. (in Polish) Warszawa 1980.
14. Rokicki E., Lindstedt P., Manerowski J., Sychała J.: The concept of monitoring blades of rotor machines with the identifications of their vibration frequency. Journal of Konbin, No. 44, 2017, DOI 10.1515/jok-2017-0080.
15. Szopliński Z.: Badanie i projektowanie układów regulacji. WNT. (in Polish) Warszawa 1975.